**Atmospheric
Chemistry
and Physics
Discussions**

Aerosol-cloud interaction determined by both in situ and satellite data over a northern high-latitude site

H. Lihavainen[1], V.-M. Kerminen[1], and L. A. Remer[2]

[1]Finnish Meteorological Institute, P.O. Box 503, 00101, Helsinki, Finland
[2]NASA Goddard Space Flight Center, Greenbelt, MD, 20771, USA

Correspondence to: H. Lihavainen (heikki.lihavainen@fmi.fi)

27465

Abstract

The first aerosol indirect effect over a clean, northern high-latitude site was investigated by determining the aerosol cloud interaction (ACI) using three different approaches; ground-based in situ measurements, combined ground-based in situ measurements 5 and satellite retrievals and using only satellite retrievals. The obtained values of ACI were highest for in situ ground-based data, clearly lower for combined ground-based and satellite data, and lowest for data relying solely on satellite retrievals. One of the key findings of this study was the high sensitivity of ACI to the definition of the aerosol burden. We showed that at least a part of the variability in ACI can be explained by 10 how different investigators have related different cloud properties to "aerosol burden".

1 Introduction

Atmospheric aerosol particles influence clouds, and thereby the Earth's climate, by altering the albedo, lifetime and precipitation patterns of clouds (e.g. Twomey, 1974; Lohmann and Feichter, 2005; Stevens and Feingold, 2009). Collectively, these effects 15 are called aerosol indirect effects. The first aerosol indirect refers to the situation in which a cloud liquid path is held constant and additional particles are introduced into the cloud, resulting in more numerous but smaller cloud droplets and a more reflective cloud.

The magnitude of the first indirect effect in the global atmosphere is poorly quantified 20 (Lohman and Feichter, 2005; Penner et al., 2006; Quaas et al., 2008). One of the main reasons for this is that the response of cloud droplet number concentration to aerosol perturbations depends in a complicated manner on both aerosol properties and prevailing meteorological conditions (e.g. Shao and Liu, 2009). Experimentally, the first indirect effect can be determined most easily by using the concept of aerosol cloud 25 interaction (ACI) that relates the cloud optical depth, droplet effective radius or droplet number concentration to the aerosol burden (Feingold et al., 2001). The magnitude

of ACI can be determined based on either in situ or remote sensing data, or on any combination of these two.

In this study, we will investigate the first indirect effect over a clean, northern high-latitude site. By determining the aerosol cloud interaction (ACI) using three different approaches that rely on ground-based in situ measurements and satellite retrievals, we are searching for an answer to the following questions: (1) can we detect the first indirect effect by all these methods at our site?, (2) do these methods produce similar values for ACI, and if not, why?, (3) is the value of ACI affected by the definition of aerosol burden, and (4) what implications our findings might have on future studies on this subject.

2 Materials and methods

2.1 Measurements

The data analyzed here include different data sets and approaches. Some of these have been published elsewhere, so only a brief description is given here. A general overview of the ground site and typical conditions there has been given by Hatakka et al. (2003).

2.1.1 Ground based in-situ measurements

The data set 1, called "*Cloud cases*", is based on measurements conducted between 2000 and 2002 at the Pallas area in northern Finland (Komppula et al., 2005). The approach takes advantage of two stations with horizontal distance of 6 km at different elevations. The higher-altitude station, Sammaltunturi, is inside a cloud about 5% of the time, whereas the lower-altitude station, Matorova, is always below the cloud layer. There are two similar Differential Mobility Particle Sizer (DMPS) measuring particles in a dry size range 7–500 nm with 30 discrete size bins. The size distribution analyzed

here are for individual cloud cases lasting from a few hours to a few days. The measurement systems and data analyses have been described in detail by Komppula et al. (2005).

The data set 2, "*First PaCE*" (The First Pallas Cloud Experiment), is based on an intensive measurement campaign carried out in the fall of 2004 in the Pallas area. The basic measurement approach is the same as in the data set "Cloud cases", but there were some additional measurements at both stations. For example, the cloud droplet number size disteribution was measured directly with a Forward Scattering Spectrometer Probe (FSSP) in Sammaltunturi. Data from the DMPS systems analyzed here are 1-h averages. More details on the measurement systems and data analyses can be found in Lihavainen et al. (2008).

The data set 3, "*Second PaCE*" (The Second Pallas Cloud Experiment), is based on an intensive measurement campaign conducted in the fall of 2005 in the Pallas area. The measurement approach is different from that during the "First PaCE" described above. The interstitial and total aerosol properties were both measured at the Sammaltunturi station using different inlet systems. The total air inlet system evaporates cloud droplets by heating. Interstitial aerosol properties were measured from a sample line that has a $PM_{2.5}$ inlet nozzle. Similar DMPS systems were attached to both lines. Additional measurements included those by an aerosol mass spectrometer and FSSP. The DMPS data analyzed here are one-hour averages. More details on the measurement systems and data analyses can be found in Anttila et al. (2009) and Kivekäs et al. (2009).

The data set 4, "*2007 Data*", was measured during a few months beginning in August 2007. The measurement system was similar to that during the "Second PaCE". The only additional measurement device was a FSSP that was running on the side with the DMPS systems. DMPS data analyzed here are one-hour averages.

2.1.2 Remote sensing and ground base measurements

For this data set (number 5), we took advantage of combining the long-term ground-based measurement at Sammaltunturi and cloud retrievals from the MODerate resolution Imaging Spectroradiometer (MODIS) on both the Aqua and Terra platforms. The data analyzed in this context covers the years 2000–2005. The cloud properties used here are an average of the 1 km×1 km retrieved effective radius and optical thickness (Platnick et al., 2003) of a 5 km×5 km box centered on the Sammaltunturi station. The data from MODIS were combined with the closest one-hour average data measured at Sammaltunturi, provided that it met the following requirements:

(a) The cloud was a low-level or boundary-layer cloud, with the limiting cloud top pressure set to 780 hPa.

(b) The liquid water path (LWP) should be constant when using the cloud droplet effective radius (r_e) or cloud optical thickness (COT) in defining the aerosol-cloud interaction (ACI, see Eqs 1 and 2 below). This was not possible due to the small number of data, so we decided to use a limited range of LWP in order to get as much data as possible. The chosen arbitrary range was from 100 to 200 g m^{-2}.

(c) The Sammaltunturi station was below the cloud base. This information we got from the visibility sensor which measures the visibility in the range from 10 m to 50 km. The limiting value for one-hour average visibility was set to 1 km.

(d) Since the ground-based data sets 1–4 are mostly from late summer and fall, the analysis here was restricted to days of year (doi) larger than 140.

(e) No rain was observed at Sammaltunturi.

2.1.3 Remote sensing

For this data set (number 6), we expanded the analysis from the local stations and took again advantage of both MODIS aerosol (Remer et al., 2005; Levy et al., 2007)

27469

and cloud (Platnick et al. 2003) retrievals from both Terra and Aqua platforms. The aerosol and cloud properties were averaged over a 1°×1° grid. The area for which the calculations were done was from 65° to 70° N and from 20° to 30° E. The time period was from 2003 to 2005. The same limiting values were applied for the cloud top pressure, seasons and LWP as for the data set 5.

2.2 Determination of the aerosol-cloud interaction

The first aerosol indirect effect is defined as the change in observed cloud optical or microphysical properties (optical depth, albedo or cloud droplet effective radius) as a function of the change in the aerosol load (e.g. Twomey, 1974). When the number concentration of aerosol particles capable of acting as cloud condensation nuclei increases, also the number concentration of cloud droplets is expected to increase. If the liquid water content of the cloud stays constant, the increase in the cloud droplet number concentration results in smaller average droplet size and thereby in a larger cloud optical depth and albedo.

The aerosol-cloud interaction (ACI) is usually calculated using one of the following relations (Feingold et al., 2001):

$$ACI = \frac{d\ln COT}{d\ln\alpha}\bigg|_{LWP} = -\frac{d\ln r_e}{d\ln\alpha}\bigg|_{LWP} = \frac{1}{3}\frac{d\ln N_d}{d\ln\alpha}.$$ (1)

Here COT is the cloud optical depth, LWP is the cloud liquid water path, r_e is the cloud droplet effective radius, N_d is number concentration of cloud droplets, and α in some proxy for the aerosol burden such as the aerosol optical depth, total number concentration of aerosol particles or aerosol light scattering coefficient. The first two partial derivatives must be calculated at the constant LWP or cloud liquid water content.

Aerosol number size distribution measurements give us an opportunity to investigate the effects of particle size on the aerosol burden and ACI. Therefore, when analysing

27470

the ground-based data, or when combining ground-based *in-situ* measurements with retrieved cloud properties from remote sensing, we used the following equation for ACI:

$$\text{ACI}(d_k) = -\left.\frac{d\,\ln r_e}{d\ln\left(\sum\limits_{i=k}^{30} N_i\right)}\right|_{\text{LWP}} = \frac{1}{3}\frac{d\,\ln A_{\text{tot}}}{d\,\ln\left(\sum\limits_{i=k}^{30} N_i\right)}.$$ (2)

Here, N_i is the number concentration of particles in the DMPS size bin i, d_k is the particle diameter in the size bin k, the index k varies between 1 ($d_1 \approx 10$ nm) and 28 ($d_{28} \approx 370$ nm), and A_{tot} is the total number concentration of aerosol particles activated to cloud droplets. Equation (2) means that we calculate ACI by using the total aerosol number concentration in the diameter range d_k to 500 nm as a proxy for the aerosol burden.

3 Results and discussion

Long-term average total particle number and sub-micron volume concentration at our measurement site are equal to $670\,\text{cm}^{-3}$ and $1.0\,\mu\text{m}^{-3}\,\text{cm}^{-3}$, respectively (Dal Maso et al., 2008). This demonstrates that the site represents a very clean continental location. Measured cloud droplet number concentrations averaged between about 130 and $180\,\text{cm}^{-3}$ for the data sets 1–4, which are at the lower end of values reported for continental clouds (Miles et al., 2002). In the following, we will apply three different methods to estimate ACI at our site and then compare the results with available literature data.

3.1 Ground-based data only

Here, we used data sets 1–4 to investigate the behavior of ACI. To start with, let us consider a lower size limit of 50–150 nm when calculating aerosol-cloud interaction. In that case, $\text{ACI}(d_k)$ varied in the range 0.2–0.3 depending on the exact value of d_k and

used data set (Fig. 1a). The correlation between different data points used to calculate ACI was high ($\sim$0.9; Fig. 1b), which is at least partly due to the fact that d_k is close to the "dry" particle diameter that separates activated cloud droplets from cloud interstitial particles at our measurement site (Komppula et al., 2005). When these two diameters are close to each other, the particle population contributing to cloud droplet activation is roughly the same as the one used to calculate the aerosol burden. Values of ACI were clearly the lowest for the data set 3 in the range d_k=50–15 nm. A major contributing factor for this feature was probably the different shape of the average particle number size distribution between the data set 3 and other data sets (Fig. 1c). Data set three 3 had also the largest variation in the accumulation mode (Fig. 1d), which may also contribute to higher ACI values at larger particle sizes.

Above 150 nm, $\text{ACI}(d_k)$ decreased rapidly with increasing d_k, reaching values between about 0.1 and 0.2 at d_k of 370 nm (Fig. 1a). The apparently lower values of ACI for d_k>150 nm do not indicate weaker aerosol-cloud interaction, but rather demonstrate that the sub-population of aerosol particles used to calculate the aerosol burden is not anymore a good representative of the one that participates in cloud droplet activation. This view is supported by simultaneous strong decrease in the correlation between different data points used to calculate ACI (Fig. 1b, exception the data set 3).

When d_k was decreased below 50 nm, values of ACI remained high, mostly above 0.25 (Fig. 1a). The main reason for this is probably that sub-50 nm particles did not give a big contribution to the total particle number concentration for the data sets 1–4 (Fig. 1c). Furthermore, the variability of the aerosol number size distribution was relatively low for these data sets (Fig. 1d).

3.2 Combined ground-based and satellite data

For the data set 5 discussed here, values of ACI were calculated using either r_e or COT obtained from satellite data as the cloud property. The aerosol burden was taken from ground-based particle number size distribution measurements in the same way as in

Sect. 3.1. After filtering the data according to the criteria given in Sect. 2.1.2, a total of 62 cases were left for further analysis.

The values of ACI for this data set were clearly lower than those obtained for data sets 1–4 (Fig. 2a), as were also the correlation coefficients between the different data points used to calculate ACI (Fig. 2b). This demonstrates that when aerosol and cloud properties are not exactly co-located, determination of aerosol-cloud interactions becomes challenging. There was also a clear, almost systematic, difference of about 0.05 in ACI when either r_e or COT was used as cloud property. A difference between these two ways of calculating ACI has been observed also in a couple of earlier studies (McComiskey et al., 2009; Pendithurai et al., 2009).

Contrary to data sets 1–4, values of ACI in the data set 5 decreased below 0.15 when the lower limit of particle sizes used to calculate the aerosol burden went below 30 nm (Fig. 2a). The probable reason for this behaviour was the relatively large number concentration of particles smaller than 30 nm and especially its large variability (Fig. 2c and d). By looking at individual particle number size distributions, particles in this size range could be traced to new-particle formation events, which is a common phenomenon around our measurement site during late summer and early fall (Dal Maso et al., 2007). This can be observed by high variation in size distributions (Fig. 2d). Practically no new-particle formation events were observed in the data sets 1–4, since the weather conditions that cause the Sammaltunturi to be within a cloud are not generally favourable to atmospheric nucleation.

3.3 Satellite data only

Here, we relied solely on satellite data for determining ACI. The values of r_e and COT were obtained as in Sect. 3.2, whereas the aerosol burden was replaced with the retrieved aerosol optical depth (AOD). A total of 505 data points were obtained when using the constraints given in Sect. 2.1.3. The data were then averaged into AOD bins of size 0.02(0–0.02, 0.02–0.04, 0.04–0.06 etc.). At least four data points in each bin were required to accept the bin to be taken into consideration.

Figure 3 shows the dependences of r_e and COT on AOD. A clear aerosol indirect effect can be seen, with of r_e decreasing and COT increasing for larger values of AOD. The value of ACI obtained from this data set was 0.1 for both r_e and COT taken as a cloud property, the respective correlation coefficients being equal to 0.45 and 0.35.

Interestingly, the value of ACI obtained for this data set is not very far from the values of ACI(d_k) in data sets 1–4 when taken 370 nm as the smallest size (d_k) to calculate the aerosol burden. The explanation for this can be found when looking at how optical measures of the aerosol burden, such as the aerosol scattering coefficient, are related to aerosol burden determined from particle number size distributions. Aaltonen et al. (2006) investigated three years of simultaneous aerosol scattering and particle number size distribution data from our measurement site. They found that while the aerosol scattering coefficient had quite a good correlation with the total number concentration of accumulation mode particles (100–500 nm; R^2=0.60), the respective correlation was much better with the number concentration of particles >200 nm in diameter (R^2=0.85) and even better with that of >300 nm particles (R^2=0.93). By putting these pieces of information together, we may conclude that, at least in our measurement site, using the aerosol scattering coefficient (and therefore also AOD) as a measure of the aerosol burden is very likely to lead to too low values of ACI.

3.4 Comparison with other studies

The values of aerosol-cloud interaction (ACI) for our in situ ground-based measurements were mostly above 0.25 when keeping the lower size limit to calculate the aerosol burden below 100–150 nm. McComiskey and Feingold (2008) summarized results from seven different in situ airborne studies made for determining aerosol-cloud interaction. In five of these studies observed values of ACI were comparable to ours (>0.20), whereas two other studies showed clearly lower values (~0.1).

By combining in situ ground-based and satellite data, and by leaving out the smallest particles to calculate the aerosol burden, we obtained ACI in the range of 0.10–0.14 when using r_e as a cloud property and in the range of 0.16–0.20 when using COT as a

cloud property. A few other studies have determined ACI with the help of ground-based remote sensing of clouds and aerosol scattering coefficient measurements. Those of them that used r_e as a cloud property, reported values of ACI that were in the range of 0.13–0.19 for Arctic clouds (Garret et al., 2004), in the ranges of 0.02–0.16 (Feingold et al., 2003) and 0.04–0.17 (Kim et al., 2008) for continental clouds, and in the range of 0.02–0.18 for marine stratus clouds (Pandithurai et al., 2009). Corresponding ranges of ACI when using COT as a cloud property have been found as 0.05–0.16 for coastal marine clouds McComiskey et al. (2009) and 0.01–0.15 for marine stratus clouds (Pandithurai et al., 2009). Taken together, these measurements indicate that the combined use of remote sensing and in situ data results in value of ACI that (i) have a relatively large variability even for the same environment, (ii) are almost always smaller than 0.20, and (iii) are clearly lower than ACI obtained from in situ measurements.

At our site, ACI determined using the satellite data was equal to 0.1 regardless of whether r_e or COT was used as a cloud property. Other satellite-based investigations have observed quite a variable range of values for ACI over different world regions (see Bulgin et al., 2008, and references therein). However, when averaging over the globe, Bulgin et al. (2008) found ACI to be in the range 0.10–0.16 during different seasons. This is line with our finding and suggests that satellite-derived values of ACI tend to be lower than those obtained using either solely by in situ data or a combination of in situ and remote sensing data.

4 Conclusions

In this work, we investigated the first indirect effect, or aerosol-cloud interaction (ACI), over a clean, northern high-latitude site using three different approaches. All of the approaches used were able to detect the first indirect effect at our site. The obtained values of ACI were highest for in situ ground-based data, clearly lower for combined ground-based and satellite data, and lowest for data relying solely on satellite retrievals. This feature is consistent with available literature data, even though it must be kept in

mind that observed values of ACI display usually a large variability even for a single site.

Perhaps the most important of our findings was the high sensitivity of ACI to the definition of the aerosol burden. For our in situ data ACI was typically at its maximum when the sub-population of aerosol particles used to calculate the aerosol burden was roughly the same as the one participating in cloud droplet activation, which meant counting all particles down to about 100 nm in diameter. Optical measures of the aerosol burden do not usually fulfil this requirement so, at least for our site, using the aerosol scattering coefficient or AOD as a measure of aerosol burden would result in values of ACI that are smaller than the "real" aerosol-cloud interaction.

Besides the aerosol burden, there are number of other factors that might affect the first indirect, or the variability of ACI as determined from measurements. One influencing factor, observed also in this study, is that aerosol and cloud properties are often not measured at the same place or time (e.g. Myhre et al., 2007; Shao and Liu, 2009). It is also well known that the fraction of aerosol particles activating into cloud droplets depends on the air updraft velocity, shape of the particle size distribution and chemical composition of the aerosol population (e.g. McFiggans et al., 2006; Reutter et al., 2009). We observed a clear effect of the shape of the particle size distribution on the magnitude of ACI.

McComiskey and Feingold (2008) made radiative forcing calculations and estimated that narrowing the uncertainty in measures of ACI to an accuracy of 0.05 would place estimated cloud radiative forcing on "a sounder footing". This sounds challenging, especially when given the large variability in reported values of ACI. We have shown that at least a part of the variability in ACI can be explained by how different investigators have related different cloud properties to "aerosol burden". In this regard, more studies should be dedicated to explore how well various optical measures of the aerosol burden can be used to calculate ACI in different environments.

References

Aaltonen, V., Lihavainen, H., Kerminen, V.-M., Komppula, M., Hatakka, J., Eneroth, K., Kulmala, M., and Viisanen, Y.: Measurements of optical properties of atmospheric aerosols in Northern Finland, Atmos. Chem. Phys., 6, 1155–1164, 2009, http://www.atmos-chem-phys.net/6/1155/2009/.

Anttila, T., Vaattovaara, P., Komppula, M., Hyvärinen, A.-P., Lihavainen, H., Kerminen, V.-M., and Laaksonen, A.: Size-dependent activation of aerosols into cloud droplets at a subarctic background site during the second Pallas Cloud Experiment (2nd PaCE): method development and data evaluation, Atmos. Chem. Phys., 9, 4841–4854, 2009, http://www.atmos-chem-phys.net/9/4841/2009/.

Bulgin, C. E., Palmer, P. I., Thomas, G. E., Arnold, C. P. G., Campmany, E., Carboni, E., Grainger, R. G., Poulsen, C., Siddans, R., and Lawrence, B. N.: Regional and seasonal variations of the Twomey indirect effect as observed by the ASTR-2 satellite instrument, Geophys. Res. Lett., 35, L02822, doi:10.1029/2007GL031394, 2008.

Dal Maso, M., Sogacheva, L., Aalto, P. P., Riipinen, I., Komppula, M., Tunved, P., Korhonen, L., Suur-Uski, V., Hirsikko, A., Kurtén, T., Kerminen, V.-M., Lihavainen, H., Viisanen, Y., Hansson, H.-C., and Kulmala, M: Aerosol size distribution measurements at four Nordic field stations: identification, analysis and trajectory analysis of new particle formation bursts, Tellus, 59B, 350–361, 2007.

Dal Maso, M., Hyvärinen, A., Komppula, M., Tunved, P., Kerminen, V.-M., Lihavainen, H., Viisanen, Y., Hansson, H.-C., and Kulmala, M.: Annual and interannual variation in boreal forest aerosol particle number and volume concentration and their connection to particle formation, Tellus, 60B, 495–508, 2008.

Feingold, G., Remer, L. A., Rmaprasad, J., and Kaufman, Y. J.: Analysis of smoke impact on

clouds in Brazilian biomass burning regions: An extention of Twomey's approach, J. Geophys. Res., 106, 22907–22922, 2001.

Feingold, G., Eberhard, W. L., Veron, D. E., and Previdi, M.: First measurements of the Twomey indirect effect using ground-based remote sensors, Geophys. Res. Lett., 30, 1287, doi:10.1029/2002GL016633, 2003.

Garrett, T. J., Zhao, C., Dong, X., Mace, G. G., and Hobbs, P. V.: Effects of varying aerosol regimes on low-level Arctic stratus, Geophys. Res. Lett., 31, L17105, doi:10.1029/2004GL019928, 2004.

Hatakka, J., Aalto, T., Aaltonen, V., Aurela, M., Hakola, H., Komppula, M., Laurila, T., Lihavainen, H., Paatero, J., Salminen, K., and Viisanen, Y.: Overview of the atmospheric research activities and results at Pallas GAW station, Boreal Environ. Res., 8, 365–384, 2003.

Kim, B.-G., Schwartz, S. E., Miller, M. A., and Min, Q.: The role of adiabaticity in the aerosol first indirect effects, J. Geophys. Res., 113, D05210, doi:10.1029/2007JD008961, 2008.

Kivekäs, N., Kerminen, V.-M., Raatikainen, T., Vaattovaara, P., Laaksonen, A., and Lihavainen, H.: Physical and chemical characteristics of aerosol particles and cloud-droplet activation during the Second Pallas Cloud Experiment (Second PaCE), Boreal Environ. Res., 14, 515–526, 2009.

Komppula, M., Lihavainen, H., Kerminen, V.-M., Kulmala, M., and Viisanen, Y.: Measurements of cloud droplet activation of aerosol particles at a clean subarctic background site, J. Geophys. Res., 110, D06204, doi:10.1029/2004JD005200, 2005.

Levy, R. C., Remer, L., Mattoo, S., Vermote, E., and Kaufman, Y. J.: Second-generation algorithm for retrieving aerosol properties over land from MODIS spectral reflectance, J. Geophys. Res., 112, D13211, doi:10.1029/2006JD007811, 2007.

Lohmann, U. and Feichter, J.: Global indirect aerosol effects: a review, Atmos. Chem. Phys., 5, 715–737, 2005, http://www.atmos-chem-phys.net/5/715/2005/.

Mauger, G. S. and Norris, J. R.: Meteorological bias in satellite estimates of aerosol-cloud relationships, Geophys. Res. Lett., 34, L16824, doi:10.1029/2007GL029952, 2007.

McComiskey, A. and Feingold, G.: Quantifying error in the radiative forcing of the first indirect effect, Geophys. Res. Lett. 35, L02810, doi:10.1029/2007GL032667, 2008.

McComiskey, A., Feingold, G., Frisch, A. S., Turner, D. D., Miller, M. A., Chiu J. C., Min Q., and Ogren J.A.: An assessment of aerosol-cloud interaction in marine stratus clouds based

on surface remote sensing, J. Geophys. Res., 114, D09203, doi:10.1029/2008JD011006, 2009.

McFiggans, G., Artaxo, P., Baltensperger, U., Coe, H., Facchini, M. C., Feingold, G., Fuzzi, S., Gysel, M., Laaksonen, A., Lohmann, U., Mentel, T. F., Murphy, D. M., O'Dowd, C. D., Snider, J. R., and Weingartner, E.: The effect of physical and chemical aerosol properties on warm cloud droplet activation, Atmos. Chem. Phys., 6, 2593–2649, 2006

Miles, N. L., Verlinde, J., and Clothiaux, E. E.: Cloud droplet size distributions in low-level stratiform clouds, J. Atmos. Sci., 57, 295–311, 2002.

Myhre, G., Stordal, F., Johnsrud, M., Kaufman, Y. J., Rosenfeld, D., Storelvmo, T., Kristjansson, J. E., Berntsen, T. K., Myhre, A., and Isaksen, I. S. A.: Aerosol-cloud interaction inferred from MODIS satellite data and global aerosol models, Atmos. Chem. Phys., 7, 3081–3101, 2007, http://www.atmos-chem-phys.net/7/3081/2007/.

Pandithurai, G., Takamura, T., Yamaguchi, J, Miyagi, K., Takano, T., Ishizaka, Y., Dipu, S., and Shimizu, A.: Aerosol effects on cloud droplet size as monitored from surface-based remote sensing over East China Sea Region, Geophys. Res. Lett., 36, L13805, doi:10.1029/2009GL038451, 2009.

Penner, J. E., Quaas, J., Storelvmo, T., Takemura, T., Boucher, O., Guo, H., Kirkevåg, A., Kristjánsson, J. E., and Seland, Ø.: Model intercomparison of indirect aerosol effects, Atmos. Chem. Phys., 6, 3391–3405, 2006, http://www.atmos-chem-phys.net/6/3391/2006/.

Platnick, S., King, M. D., Ackerman, S. A., Menzel, W. P., Baum, B. A., Riedi, J. C., and Frey, R. A.: The MODIS cloud products: Algorithms and examples from Terra, IEEE T. Geosci. Remote, 41(2), 459–473, 2003.

Quaas, J., Boucher, O., Bellouin, N., and Kinne, S.: Satellite-based estimate of the direct and indirect aerosol climate forcing, J. Geophys. Res., 113, D05204, doi:10.1029/2007JD008962, 2008.

Remer, L. A., Kaufman, Y. J., Tanre, D., Mattoo, S., Chu, D. A., Martins, J. V., Li, R. R., Ichoku, C., Levy, R. C., Kleidman, R. G., Eck, T. F., Vermote, E., and Holben, B. N.: The MODIS aerosol algorithm, products and validation, J. Atmos. Sci., 62, 947–973, 2005.

Reutter, P., Su, H., Trentmann, J., Simmel, M., Rose, D., Gunthe, S. S., Wernli, H., Andreae, M. O., and Pöschl, U.: Aerosol- and updraft-limited regimes of cloud droplet formation: influence of particle number, size and hygroscopicity on the activation of cloud condensation nuclei (CCN), Atmos. Chem. Phys., 9, 7067–7080, 2009,

27479

http://www.atmos-chem-phys.net/9/7067/2009/.

Shao, H. and Liu, G.: A critical examination of the observed first aerosol indirect effect, J. Atmos. Sci., 66, 1018–1032, 2009.

Stevens, B. and Feingold, G.: Untangling aerosols effects on clouds and precipitation in a buffered system, Nature, 461, 607–613, doi:10.1038/nature08281, 2009.

Twomey, S.: Pollution and the planetary albedo, Atmos. Environ., 8, 1251–1256, 1974.
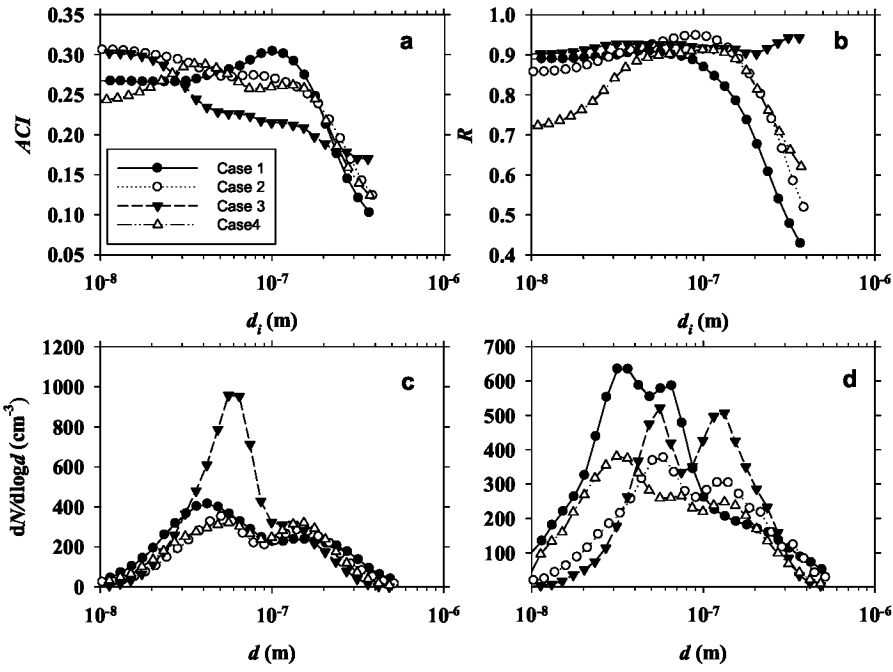
Fig. 1. (a) Aerosol-cloud interaction (ACI) in different cases as a function size where the sum of aerosol burden for ACI is taken from. **(b)** Correlation coefficient (*R*) as a function of size where the sum of aerosol burden for ACI is taken from. **(c)** Average particle number size distribution in different cases. **(d)** Standard deviation of the particle number size distribution in each case.
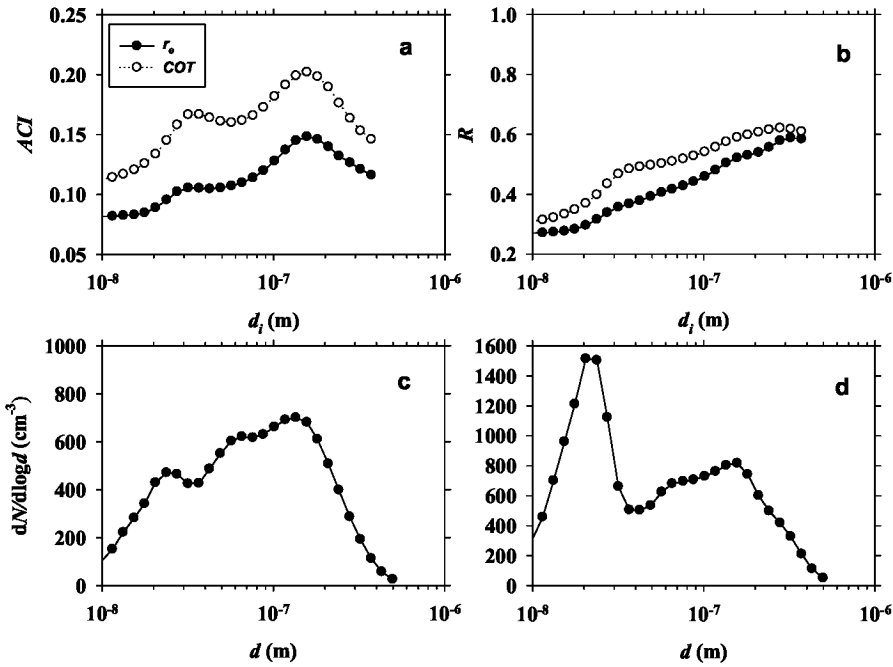
Fig. 2. (a) Aerosol-cloud interaction (ACI), as a function size where the sum of aerosol burden for ACI is taken from. **(b)** Correlation coefficient (*R*) as a function of size where the sum of aerosol burden for ACI is taken from. **(c)** Average particle number size distribution. **(d)** Standard deviation of the particle number size distribution.
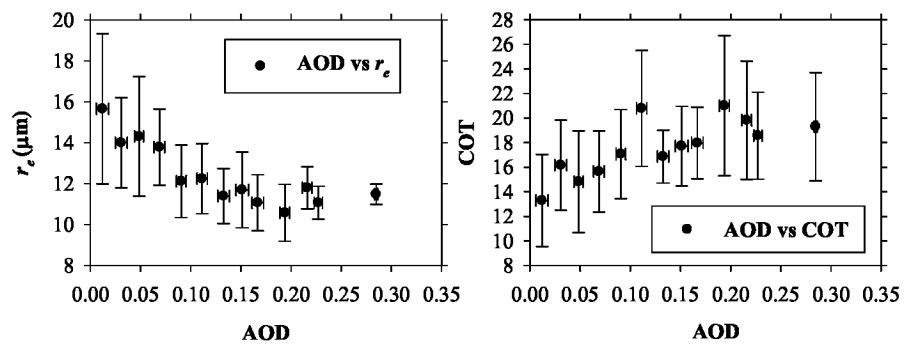
Fig. 3. On the left is the cloud is droplet effective radius (r_e) as a function of AOD. On the right is cloud optical thickness (COT) as a function of AOD. Data are based on satellite retrievals.

27483